Title

Linear energy transfer weighted beam orientation optimization for intensity-modulated proton therapy

Journal

Medical Physics, 48(1)

ISSN

0094-2405

Authors

Gu, Wenbo
Ruan, Dan
Zou, Wei
et al.

Publication Date

2021

DOI

10.1002/mp.14329

Peer reviewed

HHS Public Access

Author manuscript

Med Phys. Author manuscript; available in PMC 2022 January 01.

Published in final edited form as:

Med Phys. 2021 January ; 48(1): 57–70. doi:10.1002/mp.14329.

Linear Energy Transfer Weighted Beam Orientation Optimization for Intensity-Modulated Proton Therapy

Wenbo Gu[1], **Dan Ruan**[1], **Wei Zou**[2], **Lei Dong**[2], **Ke Sheng**[1]

[1]Department of Radiation Oncology, University of California—Los Angeles, Los Angeles, CA, 90095, USA

[2]Department of Radiation Oncology, University of Pennsylvania, Philadelphia, PA 19104, USA

Abstract

Purpose: In IMPT, unaccounted-for variation in biological effectiveness contributes to the discrepancy between the constant relative biological effectiveness (RBE) model prediction and experimental observation. It is desirable to incorporate biological doses in treatment planning to improve modeling accuracy and consequently achieve a higher therapeutic ratio. This study addresses this demand by developing a method to incorporate linear energy transfer (LET) into beam orientation optimization (BOO).

Methods: Instead of RBE-weighted dose, this LET weighted BOO (LETwBOO) framework uses the dose and LET product (LET×D) as the biological surrogate. The problem is formulated with a physical dose fidelity term, a LET×D constraint term, and a group sparsity term. The LET×D of OARs are penalized for minimizing the biological effect while maintaining the physical dose objectives. Group sparsity is used to reduce the number of active beams from 600–800 non-coplanar candidate beams to between 2 and 4. This LETwBOO method was tested on three skull-base tumor (SBT) patients and three bilateral head-and-neck (H&N) patients. The LETwBOO plans were compared with IMPT plans using manually selected beams with only physical dose constraint (MAN) and the initial MAN plan reoptimized with additional LET×D constraint (LETwMAN).

Results: The LETwBOO plans show superior physical dose and LET×D sparing. On average, the [mean, maximal] doses of OARs in LETwBOO are reduced by [2.85, 4.6] GyRBE from the MAN plans in the SBT cases and reduced by [0.9, 2.5] GyRBE in the H&N cases, while LETwMAN is comparable to MAN. cLET×Ds of PTVs are comparable in LETwBOO and LETwMAN, where c is a scaling factor of 0.04 μm/keV. On average, in the SBT cases, LETwBOO reduces the OAR [mean, maximal] cLET×D by [1.1, 2.9] Gy from the MAN plans, compared to the reduction by LETwMAN from MAN of [0.7, 1.7] Gy. In the H&N cases, LETwBOO reduces the OAR [mean, maximal] cLET×D by [0.8, 2.6] Gy from the MAN plans, compared to the reduction by LETwMAN from MAN of [0.3, 1.2] Gy.

Corresponding author: Ke Sheng, Ph.D., UCLA Radiation Oncology, 200 Medical Plaza Driveway, Los Angeles, CA, 90095, USA, ksheng@mednet.ucla.edu.

Disclosure of Conflicts

The authors have no relevant conflicts of interest to disclose.

Conclusion: We developed a novel LET weighted BOO method for IMPT to generated plans with improved physical and biological OAR sparing compared with the plans unaccounted for biological effects from BOO.

1. Introduction

In current proton therapy clinical practice, a constant relative biological effectiveness (RBE) value of 1.1 is used [1–3]. However, the generic RBE of 1.1 is an averaged value at the center of a spread-out Bragg peak (SOBP) for 65–250 MeV proton of in-vivo systems[2]. The RBE can vary substantially along with treatment fields (ranging from 1.0 to 1.6 in SOBP)[4]. RBE values depend on several other factors, such as linear energy transfer (LET), tissue radiobiological properties (α and β value), physical dose, and specific biological endpoint[2,4,5].In addition, with the pencil beam scanning (PBS) technique replacing passive scattering to be the mainstream delivery modality, the biological doses potentially differ from the previous observation on passive scattering[6,7], warranting further investigation in the universal use of RBE=1.1.

There have been concerns that using the generic RBE value in proton therapy can lead to underdosage in the target or underestimation of the normal tissue toxicities. Several empirical RBE calculation models have been proposed[5,8–11] to more accurately predict the RBE values. Efforts have then been made to include the RBE-weighted dose into treatment planning[12–15]. However, the dependence of these models on fitting parameters and tissue radiobiological properties introduces considerable uncertainties in RBE-weighted dose prediction, making it difficult to incorporate them into clinical treatment planning.

Alternatively, dose-averaged LET has been suggested as a surrogate for indirect biological optimization[16]. The increase of biological effectiveness from the entrance to the distal edge of the Bragg peak is largely due to the increase of LET towards the end of the proton range. Although the relationship is nonlinear, RBE increases monotonically with LET[4,5,8–11], making LET a reasonable first-order approximation of RBE. Moreover, in contrast to the large RBE estimation uncertainties, LET can be accurately calculated via analytical modeling[17–20] or Monte Carlo simulation[21–24]. The LET values can then be utilized in multi-field optimized Intensity-Modulated Proton Therapy (MFO-IMPT, shorted as IMPT)[25,26].

Studies have been performed to incorporate dose-averaged LET into biological optimization of IMPT. Tseung et al[27] and Fager et al[28] used LET painting to directly optimize the biological dose instead of the physical dose, which was considered impractical. A safer and more acceptable strategy is to simultaneously optimize LET and physical dose. Works have been done to maximize the LET in the target or minimize the LET in the critical organs at risk (OARs), while achieving the physical prescription doses in the target and the OARs[25,29–34]. For example, Unkelbach et al[25] suggested reoptimizing the product of LET and physical dose (LET×D) after obtaining an initial IMPT plan based on the physical dose. They showed reduced LET hot spots in the critical structures with little physical dose degradation.

However, existing LET or LET×D optimization is limited to fixed beams despite the significant implication of beam orientations on the LET distribution[25,29,35–37]. For example, if an OAR abuts the target in the distal edge of a proton beam, it is difficult to reduce the LET in this OAR without compromising physical dose coverage. In clinical practice, a planner can avoid some of the undesirable beam orientations based on experience[29,35–37], but evaluating all beam angles for their dosimetry, robustness, and LET values is a large computational task unsuited for human operators. A beam orientation optimization (BOO) algorithm for both physical and biological dose optimization is essential for IMPT but has not been developed.

We previously developed an automated IMPT BOO algorithm using group sparsity regularization for physical dose objectives[38,39]. IMPT BOO automatically selects beam angles and creates treatment plans with superior physical dose distribution to human expert-created plans. In this work, we expand the group sparsity BOO framework for IMPT biological dose optimization.

2. Materials and Methods

The general goal of our IMPT BOO algorithms is to select 2~4 beams out of all candidate beams and simultaneously generate the fluence map of the selected beams with certain objectives. The beam selection is achieved by group sparsity regularization. In the previously developed BOO algorithm[38,39], physical dose conformality is selected as the optimization objective. In this Linear Energy Transfer weighted Beam Orientation Optimization (LETwBOO) framework, biological sparing is achieved as an optimization weight on the physical dose constraints.

In this LETwBOO method, the dose and LET product (LET×D) is used as a surrogate of biological effectiveness. This LETwBOO method aims to select proton beams and generate treatment plans with superior physical dose distribution and LET×D sparing in the OARs. The optimization function is formulated with a dose fidelity term, a LET×D constraint term, and a group sparsity term. The details are described as follows.

2.1. Dose and LET product

As proposed by Unkelbach et al[25], the RBE-weighted dose at voxel i, written as BD_i, can be approximated by:

$$BD_i = D_i + cLD_i, \tag{1}$$

where D_i is the physical dose delivered to voxel i, LD_i is the dose and LET product at voxel i, and c is a scaling factor. The two terms represent the physical and LET weighted doses, respectively. The scaling factor c value is assumed 0.04 μm/keV following the publication[25].

In order to formulate the optimization problem, two matrices, A and L, are first defined. The matrix A is the dose calculation matrix, to transform the spot intensities to the dose delivered to the patient volume. The element in the ith row and jth column of matrix A, denoted as a_{ij}, representing the physical dose contribution from the pencil beam j of unit intensity to the

voxel i. Matrix L is the LET calculation matrix. Similar to A, the ijth element in L, denoted as l_{ij}, is the LET from the pencil beam j to the voxel i of unit intensity. Let $\boldsymbol{x}$ be a vector representing the intensities of all the scanning spots, with x_j indicating the intensity of jth spot, then the physical dose to voxel i from all scanning spots is calculated as

$$D_i = \sum_j a_{ij} x_j \,. \tag{2}$$

The dose-averaged LET to voxel i over all scanning spots is

$$LET_i = \frac{1}{D_i} \sum_j l_{ij} a_{ij} x_j \,. \tag{3}$$

Therefore, the product of dose and LET at voxel i is:

$$LET_i \times D_i = \sum_j l_{ij} a_{ij} x_j \,. \tag{4}$$

In matrix-vector representation, the vectorized physical dose in the patient volume denoted as D, can be written as

$$D = A\boldsymbol{x} \,. \tag{5}$$

The product of dose and LET in the patient volume denoted as LD, can be calculated as the following matrix and vector multiplication:

$$LD = (L \circ A)\boldsymbol{x}, \tag{6}$$

where the symbol '$\circ$' represents element-wise multiplication.

2.2. Problem formulation

In the LETwBOO framework, the LET×D constraint is incorporated into the group sparsity based BOO to encourage selecting proton beams which minimize LET×D in the OARs, while maintaining LET×D to the target as well as achieving superior physical dose distribution. Assume $\mathscr{B}$ is the set containing all the feasible candidate beams. The LETwBOO problem is formulated as

$$\begin{aligned} \underset{\boldsymbol{x}}{\text{minimize}} \; & \sum_{k \in \mathscr{T}} \alpha_k \| A_k \boldsymbol{x} - p_k \|_2^2 + \sum_{k \in \mathscr{O}} \alpha_k \| A_k \boldsymbol{x} \|_2^2 \\ & + \sum_{k \in \mathscr{T}} \beta_k \left\| ((LD)_k^{\text{ref}} - (L \circ A)_k \boldsymbol{x})_+ \right\|_2^2 + \sum_{k \in \mathscr{O}} \beta_k \| (L \circ A)_k \boldsymbol{x} \|_2^2 \\ & + \sum_{b \in \mathscr{B}} \lambda_b \| \boldsymbol{x}_b \|_2^{1/2} \\ \text{subject to} \quad & \boldsymbol{x} \geq 0, \end{aligned} \tag{7}$$

where $\boldsymbol{x}_b$ is a vector representing the intensities of scanning spots from the candidate beam b, so the optimization variable $\boldsymbol{x}$ is the concatenation of all the vectors x_b ($b \in \mathscr{B}$). The dose calculation matrix A and LET calculation matrix L include all the candidate beams along the column direction. $\mathscr{T}$ is the set including the target volumes and $\mathscr{O}$ is the set including the OARs.

The first two terms in problem (7) are the conventional physical dose fidelity term. The first term penalizes the dose deviation of target k from prescription dose p_k, to ensure a homogeneous physical dose distribution in the target. The second term penalizes any non-zero doses in the OARs, to reduce the doses delivered to the OARs. The third and fourth terms together are the LET×D conditions. The third term encourages the LET×D values in the target k to be greater than $(LD)_k^{\mathrm{ref}}$, to prevent cold spots in the biological dose. $(\bullet)_+$ is an one-sided function where all the negative values are treated as zero. The fourth term minimizes the LET×D values in the OARs. α_k and β_k are the structure weighting hyperparameters for dose and LET×D constraints, respectively.

The last term $\sum_{b \in \mathscr{B}} \lambda_b \|\boldsymbol{x}_b\|_2^{1/2}$ is an $L_{2,1/2}$-norm group sparsity term. With a proper value of weighting hyperparameter for each beam b, denoted as λ_b, most $\boldsymbol{x}_b$ are penalized to be identically zero. Therefore, most candidate beams are turned off, leaving a small number (2–4) of beams active.

Without the third and fourth terms penalizing LET×D, the problem (7) is the group sparsity based BOO framework proposed in our previous work[38], only ensuring physical dose sparing. After adding these two terms, proton beam angles and treatment plans are generated simultaneously with optimum physical dose and LET×D sparing. FISTA, an accelerated proximal gradient method known as the Fast Iterative Shrinkage-Thresholding Algorithm[40] is used to solve this non-differentiable problem.

2.3. Evaluations

Three patients with skull base tumor (SBT) and three patients with bilateral head-and-neck (H&N) cancer were tested. The original candidate beam set included 1162 non-coplanar beams, which were evenly distributed across the 4π space with 6° separation. Among the candidate beams, geometrically undesired beams and beams of infeasible energies, such as those directed through the feet to the head, were manually excluded from the candidate set, resulting in 700 to 800 candidate beams for the SBT patients and approximately 600 beams for the H&N patients. More accurate beam screening can be performed for a specific proton gantry but should not affect the generality of the current study. For each candidate beam, dose and LET calculation for the scanning spots covering the PTV (planning target volume) and a 5 mm margin was performed by matRad v2.1.0[41,42], a MATLAB-based 3D treatment planning toolkit. The dose calculation matrix A and LET calculation matrix L including all feasible candidate beams were hence generated. The calculation resolution was 2.5×2.5×2.5 mm^3. Since robust optimization is not considered in this work yet, the PTV was set as the optimization target. The prescription dose, target volume, and average spot count per beam for each patient are shown in Table I.

For comparison, in addition to the LETwBOO plan, the following four plans were also generated for each patient: 1) conventional plan optimizing physical dose with manually selected beams (MAN); 2) the same MAN plan reoptimized with additional cLET×D constraint (LETwMAN); 3) the plan generated by group sparsity based BOO with only physical dose constraint (GSBOO); 4) the same GSBOO plan reoptimized with additional cLET×D constraint (GSBOO_LETwFMO, with FMO representing fluence map optimization). The differences of these plans are listed in Table II.

MatRad is used in this work to generate the pencil beam dose and LET data for all plans in an acceptable time. The analytical method is limited in accuracy but separable from the proposed LETwBOO framework, which can be generalized to use other dose and LET calculation engines, including the more accurate but significantly slower Monte Carlo methods. To demonstrate the generality, MCsquare v1.1, a many-core Monte Carlo simulation tool[43,44] is also tested for planning. Due to the long time (several days for cases with a small tumor and two weeks for medium-sized tumor cases) needed to calculate the dose and LET of every pencil beam of all candidate beams, the additional Monte Carlo based planning was limited to SBT #3, where 1×10^6 primary proton particles per pencil beam were simulated using MCsquare.

For all plans, the goal of physical dose optimization is the same as conventional treatment planning. We set the physical dose distribution in the target to be homogeneous and a constant RBE value of 1.1 was used. The plans are normalized so that 95% of the target volume receives the prescribed physical dose, which is $\frac{\text{prescription dose}}{1.1}$. For the biological component, since there is no predefined reference value for cLET × D that can be used, we set the $c(LD)^{\text{ref}}$ of the PTVs to the mean cLET × D value of the PTVs in the MAN plans.

PTV homogeneity, D95%, and maximum dose were evaluated. PTV homogeneity is defined as D95%/D5%. The maximum dose is defined as the dose to 2% of the structure volume, D2%, following the recommendation by IRCU-83[47]. The mean and maximum doses for OARs were also evaluated. In addition, the mean and maximum cLET×D for the PTVs and OARs are evaluated to compare the biological effectiveness.

3. Results

3.1. Runtime and selected beams

The calculation and optimization were performed on a Xeon 14-core CPU server operating at 2.40 GHz clock. To calculate the dose and LET of all feasible candidate beams, the Matlab Parallel Computing Toolbox was used to accelerate the computation on matRad. The times spent on the dose and LET calculation and the BOO runtime for the GSBOO and LETwBOO plans are listed in Table III. The couch and gantry angles for the beams from manual selection, GSBOO, and LETwBOO, are also listed in Table III. In matRad, the physical dose calculation and LET calculation share the same ray-tracing procedure, which is also the most time-consuming step. Therefore, the total time for dose and LET calculation is shown. With the analytical calculation model and parallel computing, the total time for dose and LET calculation is between 10 to 60 min depending on the target size. While the

GSBOO process with only physical dose constraint took about 20–70 minutes to complete, the LETwBOO process with additional cLET×D constraint increased the BOO time by 30–80%.

3.2. SBT cases

LETwBOO is compared with MAN and GSBOO. The PTV statistics of dose and LET×D of the three SBT patients can be found in Figure 1. Qualitatively, all five methods achieved similar PTV dose coverage. In the GSBOO plans, the cLET×D values of the PTVs were not guaranteed, which can be higher (SBT #1) or lower (SBT #2) than the MAN plan. With the LET×D constraint in the LETwMAN, LETwBOO, and GSBOO_LETwFMO plans, the mean and maximal values of LET×D of the PTVs were similar compared with the MAN plans, but the minimal values of PTV LET×D were improved relative to the MAN plans.

The dose volume histograms and cLET×D volume histograms for the three SBT patients comparing MAN, LETwMAN, and LETwBOO are shown in Figure 2 and that comparing GSBOO, GSBOO_LETwFMO, and LETwBOO are shown in Figure 3. The differences in dose and LET×D of LETwMAN, GSBOO_LETwFMO, and LETwBOO plan from the MAN plan for some OARs are shown in Figure 4.

Reoptimizing the MAN plan based on the proposed LET×D constraint resulted in lower LET×D of the OARs while maintaining similar physical dose distribution. In the GSBOO plans, where only physical dose constraint was considered, the physical dose was improved, but the sparing of LET×D was not guaranteed. For example, the maximal cLET×D of the left optical nerve for SBT #1 in the GSBOO plan was 2.4 Gy higher than the MAN plan. Reoptimizing LET×D based on the GSBOO plans leads to slightly degraded physical dose distribution and lower LET×D, but the LET×D sparing was not as good as LETwMAN. On average, the GSBOO_LETwFMO plans reduced [Dmean, Dmax] from the LETwMAN plans by [3.8, 4.5] GyRBE on average, but increasing [cLET×Dmean, cLET×Dmax] by [0.1, 0.4] Gy.

The LETwBOO plans achieved better OARs dose sparing and further reduced the OARs LET×D. The physical dose was reduced in the LETwBOO plans from the MAN plan for most considered OARs except the chiasm in SBT #1 and SBT #3, and the right optical nerve in SBT #2. Even for these structures that were not improved compared with MAN, the difference was smaller than 1 GyRBE. The structure with the largest reduction in the maximal doses from the MAN plans was the left eye (9.1 GyRBE) for SBT #1, pharynx (13.8 GyRBE) for SBT #2, and hippocampus (15.7 GyRBE) for SBT #3. The averaged reduction in [Dmean, Dmax] of the LETwBOO plans from the MAN plans were [2.85, 4.6] GyRBE, while the averaged reduction of [Dmean, Dmax] of the LETwMAN plans from the MAN plans were [0.1, 0.5] GyRBE.

Meanwhile, even though the LETwBOO method did not improve the physical dose for certain structures in the SBT cases, it further reduced the LET×D compared with LETwMAN. For example, the maximal cLET×Ds of the chiasm in the three cases were 1.5 Gy, 0.9 Gy, and 1.0 Gy lower than the LETwMAN plans, respectively, while the physical doses were similar. Compared with the LETwMAN plans, the structure with the largest

reduction of maximal cLET×D by LETwBOO in each case was the right optical nerve (1.7 Gy) for SBT #1, pharynx (2.9 Gy) for SBT #2, and brainstem (1.6 Gy) for SBT #3. The averaged reduction of [cLET×Dmean, cLET×Dmax] of the LETwBOO plans from the MAN plans were [1.1, 2.9] Gy, while the averaged reduction of [cLET×Dmean, cLET×Dmax] of the LETwMAN plans from the MAN plans were [0.7, 1.7] Gy. The isodose and iso-cLET×D of one transverse plane in the SBT#3 patient are compared between MAN, LETwMAN, and LETwBOO plans and shown in Figure 5. While the LETwMAN redistributes the cLET×D to lower the values in the optical nerves and chiasm, a further reduction of cLET×D can be observed in the LETwBOO plan, as pointed out by the red arrows.

3.3. H&N cases

The PTV statics of the three H&N patients is shown in Figure 6. Similar to the SBT cases, all five methods achieved similar PTV dose coverage and comparable cLET×D distribution. An improvement of minimal cLET×D is observed in the LETwMAN, LETwBOO, and GSBOO_LETwFMO plans from the MAN plans, indicating reduced cLET×D cold spots in the PTVs.

The dose volume histograms and cLET×D volume histograms for the three H&N patients comparing MAN, LETwMAN, and LETwBOO are shown in Figure 7, and that comparing GSBOO, GSBOO_LETwFMO, and LETwBOO are shown in Figure 8. The differences in dose and LET×D of LETwMAN, GSBOO_LETwFMO, and LETwBOO plans relative to the MAN plan for selected OARs are shown in Figure 9.

Compared with LETwMAN, GSBOO_LETwFMO reduced [Dmean, Dmax] by [1.7, 2.6] GyRBE on average, with similar LET×D and an average increase of [cLET×Dmean, cLET×Dmax] by [−0.1, 0.1] Gy.

The OARs doses in the LETwBOO plans were consistently reduced compared with the MAN plans except for the right submandibular gland in H&N #1 and H&N #3. The structure of the largest reduction of maximal dose from the MAN plan in each case was right parotid (5.9 GyRBE) for H&N #1, constrictors (4.6 GyRBE) for H&N #2, and larynx (4.4 GyRBE) for H&N #3. The averaged reduction of [Dmean, Dmax] of the LETwBOO plans from the MAN plans was [0.9, 2.5] GyRBE, while the [Dmean, Dmax] of the LETwMAN plans were increased by [0.5, 0.2] GyRBE from the MAN plans.

Even though the doses to the right submandibular gland in the three LETwBOO plans were comparable to the MAN plans, an effective reduction of LET×D by the LETwBOO method was observed. Compared with the LETwMAN plans, the maximal cLET×Ds of the right submandibular gland in the three cases were 2.3 Gy, 2.2 Gy, and 1.2 Gy lower in the LETwBOO plans. The averaged reduction of [cLET×Dmean, cLET×Dmax] of the LETwBOO plans from the MAN plans were [0.8, 2.6] Gy, while the averaged reduction of [cLET×Dmean, cLET×Dmax] of the LETwMAN plans from the MAN plans were [0.3, 1.2] Gy.

3.4. Monte Carlo results

The plans optimized based on MCsquare for the SBT #3 patient are shown in Figure 10. The dose volume histograms and cLET×D volume histograms comparing MAN, LETwMAN, and LETwBOO are in Figure 10(a), and the isodose and iso-LET×D comparisons are shown in Figure 10(b). The difference in the dose and LET calculation methods resulted in different selected beam angles and final plans shown as matRad (Figure 5) and MCsquare (Figure 10). Nevertheless, LETwBOO took advantage of the Monte Carlo calculation results to further reduce the optical nerves and chiasm doses and cLET×Ds compared with LETwMAN.

It is also noted that in the MCsquare plans, the low LET×D area in the PTV6300 is larger, as shown in the cLET×D volume histograms in Figure 10(a), and pointed out by the red arrows in in Figure 10(b). Compared with MCsquare, matRad overestimated the LET values in the low-density region in the nasal cavity, which is included in the PTV.

4. Discussion

Unexpected high LET-weighted pencil beam dose deposition inside a sensitive OAR has raised considerable concerns in IMPT plans. Although the beam direction strongly correlates with the distal proton biological effect, IMPT optimization may scatter high-LET beams throughout the target volume or sometimes within OARs. Manual selection of proton fields for multiple planning goals, including optimal dosimetry, biological effectiveness, and robustness, is a computational task beyond the capability of human planners. To the best of our knowledge, this work describes the first mathematical framework and actual implementation that includes LET in IMPT beam orientation optimization. In contrast to the limited manual trial and error approach, the LETwBOO framework performs a global search among all feasible candidate beams by solving a group sparsity problem integrating physical dose objectives and biological surrogate constraints.

Compared with the previous approaches appending LET optimization to the physical dose optimization using manually selected beams, which were shown to reduce LET in the OARs at the cost of the physical dose[25], LETwBOO further reduced *both* the physical dose and LET×D in the OARs. The OAR dose and LET reduction was achieved while maintaining the physical target dose and LET×D coverage, eliminating concerns due to uncertain tumor radiobiology and RBE modeling. It is worth noting that the current framework is flexible to increase LET×D in the tumor for potentially greater tumor cell killing by setting the $(LD)^{\text{ref}}$ value in problem (7) higher.

A limitation of the current LETwBOO framework is that the reference LET×D values for targets and normal tissues are unknown. Subsequently, the $(LD)^{\text{ref}}$ and weighting hyperparameters for the LET×D constraints cannot be mechanistically determined. In this study, the $(LD)^{\text{ref}}$ value for the LETwMAN and LETwBOO plans of each patient was extracted from the corresponding conventional MAN plan so that we could compare the biological effectiveness with the MAN plan. However, in the clinical setting, the lack of reference values makes it difficult to directly use LETwBOO for a new case. A potential solution is to set a typical SOBP single field plan before treatment planning and calculate the

mean LET×D for the targets as the reference value. Another alternative solution is that templates can be built for different sites, e.g. H&N and skull base in this study. Meanwhile, further preclinical and clinical research is needed for more quantitative integration of RBE modeling in treatment planning, as recommended by AAPM TG-256[3].

In this work, (D+cLET×D) is used as a surrogate for RBE-weighted dose, which cannot be incorporated into the existing optimization framework due to its dependence on the total contribution of multiple pencil beams and the uncertain underlying biological models, which include approximately known alpha/beta values, and the varying endpoints to assess tissue toxicities. We note that LET×D is not equivalent to the biological effectiveness. However, according to experiments and RBE models[4,5,8–11], high LET×D values are correlated with a high RBE-weighted dose when other factors are fixed. Therefore, it is reasonable to minimize LET×D using the proposed LETwBOO framework to reduce the biological damage to the OARs. Moreover, instead of non-linear RBE models, incorporating linear LET×D model into the BOO algorithm makes the problem straightforward to solve using the FISTA, with an optimal convergence rate of $O(1/k^2)$ among first-order optimization methods[40].

In our current framework, the physical dose and the additional biological component represented by LET×D are optimized in two separate terms. An alternative approach of biological optimization is to directly optimize the BD shown in the Equation (1), which is regarded as a first-order approximation of RBE-weighted dose. However, the accuracy of this linear approximation is unclear, and directly optimizing BD cannot guarantee the conformality of physical dose distribution. While further investigations are needed to better understand the radiobiology of proton therapy, a method improving biological effectiveness while maintaining the physical dose objectives may be a safe and clinically acceptable solution. Therefore we placed both physical dose and LET×D constraints in the proposed framework in Equation (7).

Due to the prohibitively long time required to calculate dose and LET for over 500 candidate beams using Monte Carlo, the current study used an analytical method for all patients and limited Monte Carlo based planning to only one patient. The analytical method was shown to be acceptably accurate for dose calculation and BOO planning in our previous paper[38,39], it is limited in LET calculation accuracy due to reasons including failing to account for secondary protons[17]. The deficiency is shown as overestimation of LET in the low-density region compared with the Monte Carlo method. It is also observed that a different dose and LET calculation method can result in different optimized beams. Because LETwBOO is separable from the underlying dose and LET calculation method, it optimizes beams and intensity modulation patterns that are consistent with the dose and LET calculation. In SBT#3 planned using matRad and MCSquare, LETwBOO was able to better spare the OARs than LETwMAN in both cases.

Plan robustness is not explicitly incorporated in the current framework. The uncertainties from planning and delivery of IMPT not only affect the physical dose, but also change the RBE (LET) distribution. Biologically robust optimization algorithms have been proposed mainly based on worst-case optimization[29,33,48], which is difficult to be incorporated in the

BOO framework due to its prohibitive computational cost. Previously a sensitivity regularization was developed by our group to improve the physical dose robustness[49] of IMPT plans, and was later incorporated into a BOO framework to encouraging finding beam angles with high physical dose robustness[39]. In the future work, regularization terms modeling RBE or LET sensitivity against uncertainties will be developed and included in this LETwBOO framework, for the robustness of both physical dose and biological dose.

5. Conclusions

We developed a novel LET weighted BOO method for IMPT to generated plans with superior physical and biological OAR sparing to plans decoupling biological effects from BOO.

Acknowledgment

This research is supported by NIH Grants Nos. R44CA183390, R43CA183390, and R01CA230278.

Reference

1. Gerweck LE, Kozin SV. Relative biological effectiveness of proton beams in clinical therapy. Radiother Oncol 1999;50(2):135–142. doi:10.1016/S0167-8140(98)00092-9 [PubMed: 10368035]
2. Paganetti H, Niemierko A, Ancukiewicz M, et al. Relative biological effectiveness (RBE) values for proton beam therapy. Int J Radiat Oncol Biol Phys 2002;53(2):407–421. doi:10.1016/S0360-3016(02)02754-2 [PubMed: 12023146]
3. Paganetti H, Blakely E, Carabe-Fernandez A, et al. Report of the AAPM TG-256 on the relative biological effectiveness of proton beams in radiation therapy. Med Phys 2019. doi:10.1002/mp.13390
4. Paganetti H Relative biological effectiveness (RBE) values for proton beam therapy. Variations as a function of biological endpoint, dose, and linear energy transfer. Phys Med Biol 2014;59(22):R419–R472. doi:10.1088/0031-9155/59/22/R419 [PubMed: 25361443]
5. McNamara AL, Schuemann J, Paganetti H. A phenomenological relative biological effectiveness (RBE) model for proton therapy based on all published in vitro cell survival data. Phys Med Biol 2015;60(21):8399–8416. doi:10.1088/0031-9155/60/21/8399 [PubMed: 26459756]
6. Gridley DS, Pecaut MJ, Mao XW, Wroe AJ, Luo-Owen X. Biological Effects of Passive Versus Active Scanning Proton Beams on Human Lung Epithelial Cells. Technol Cancer Res Treat 2013;14(1):81–98. doi:10.7785/tcrt.2012.500392
7. Mishra M V, Khairnar R, Bentzen SM, et al. Proton beam therapy delivered using pencil beam scanning vs. passive scattering/uniform scanning for localized prostate cancer: Comparative toxicity analysis of PCG 001–09. Clin Transl Radiat Oncol 2019;19:80–86. doi:10.1016/j.ctro.2019.08.006 [PubMed: 31650043]
8. Wilkens JJ, Oelfke U. A phenomenological model for the relative biological effectiveness in therapeutic proton beams. Phys Med Biol 2004;49(13):2811–2825. doi:10.1088/0031-9155/49/13/004 [PubMed: 15285249]
9. Carabe-Fernandez A, Dale RG, Jones B. The incorporation of the concept of minimum RBE (RbEmin) into the linear-quadratic model and the potential for improved radiobiological analysis of high-LET treatments. Int J Radiat Biol 2007;83(1):27–39. http://www.ncbi.nlm.nih.gov/pubmed/17357437. [PubMed: 17357437]
10. Wedenberg M, Lind BK, Hårdemark B. A model for the relative biological effectiveness of photons is a predictor for the sensitivity to LET changes. Acta Oncol (Madr) 2012;52(June 2012):1–9. doi:10.3109/0284186X.2012.705892

11. Jones B, McMahon SJ, Prise KM. The Radiobiology of Proton Therapy: Challenges and Opportunities Around Relative Biological Effectiveness. Clin Oncol 2018;30(5):285–292. doi:10.1016/j.clon.2018.01.010
12. Wilkens JJ, Oelfke U. Optimization of radiobiological effects in intensity modulated proton therapy. Med Phys 2005;32(2):455–465. doi:10.1118/1.1851925 [PubMed: 15789592]
13. Frese MC, Wilkens JJ, Huber PE, Jensen AD, Oelfke U, Taheri-Kadkhoda Z. Application of constant vs. variable relative biological effectiveness in treatment planning of intensity-modulated proton therapy. Int J Radiat Oncol Biol Phys 2011;79(1):80–88. doi:10.1016/j.ijrobp.2009.10.022 [PubMed: 20382482]
14. Guan F, Geng C, Ma D, et al. RBE model-based biological dose optimization for proton radiobiology studies. Int J Part Ther 2019. doi:10.14338/IJPT-18-00007.1
15. Takada K, Sato T, Kumada H, et al. Validation of the physical and RBE-weighted dose estimator based on PHITS coupled with a microdosimetric kinetic model for proton therapy. J Radiat Res 2018. doi:10.1093/jrr/rrx057
16. Grassberger C, Paganetti H. Elevated LET components in clinical proton beams. Phys Med Biol 2011;56(20):6677–6691. doi:10.1088/0031-9155/56/20/011 [PubMed: 21965268]
17. Wilkens JJ, Oelfke U. Analytical linear energy transfer calculations for proton therapy. Med Phys 2003;30(5):806–815. doi:10.1118/1.1567852 [PubMed: 12772988]
18. Wilkens JJ, Oelfke U. Three-dimensional LET calculations for treatment planning of proton therapy. Z Med Phys 2004. doi:10.1078/0939-3889-00191
19. Sanchez-Parcerisa D, Cortés-Giraldo MA, Dolney D, Kondrla M, Fager M, Carabe A. Analytical calculation of proton linear energy transfer in voxelized geometries including secondary protons. Phys Med Biol 2016;61(4):1705–1721. doi:10.1088/0031-9155/61/4/1705 [PubMed: 26840945]
20. Hirayama S, Matsuura T, Ueda H, et al. An analytical dose-averaged LET calculation algorithm considering the off-axis LET enhancement by secondary protons for spot-scanning proton therapy. Med Phys 2018. doi:10.1002/mp.12991
21. Cortés-Giraldo MA, Carabe A. A critical study of different Monte Carlo scoring methods of dose average linear-energy-transfer maps calculated in voxelized geometries irradiated with clinical proton beams. Phys Med Biol 2015. doi:10.1088/0031-9155/60/7/2645
22. Perl J, Shin J, Faddegon B, Paganetti H. TOPAS : An innovative proton Monte Carlo platform for research. Med Phys 2012;39(11):6818–6837. 10.1118/1.4758060. [PubMed: 23127075]
23. Grzanka L, Ardenfors O, Bassler N. Monte carlo simulations of spatial let distributions in clinical proton beams. Radiat Prot Dosimetry 2018. doi:10.1093/RPD/NCX272
24. Qin N, Botas P, Giantsoudi D, et al. Recent developments and comprehensive evaluations of a GPU-based Monte Carlo package for proton therapy. Phys Med Biol 2016. doi:10.1088/0031-9155/61/20/7347
25. Unkelbach J, Botas P, Giantsoudi D, Gorissen B, Paganetti H. Reoptimization of intensity-modulated proton therapy plans based on linear energy transfer. Int J Radiat Oncol Biol Phys 2016;96(5):1097–1106. doi:10.1016/J.IJROBP.2016.08.038 [PubMed: 27869082]
26. Grassberger C, Trofimov A, Lomax A, Paganetti H. Variations in linear energy transfer within clinical proton therapy fields and the potential for biological treatment planning. Int J Radiat Oncol Biol Phys 2011;80(5):1559–1566. doi:10.1016/j.ijrobp.2010.10.027 [PubMed: 21163588]
27. Wan Chan Tseung HS, Ma J, Kreofsky CR, Ma DJ, Beltran C. Clinically Applicable Monte Carlo–based Biological Dose Optimization for the Treatment of Head and Neck Cancers With Spot-Scanning Proton Therapy. Int J Radiat Oncol Biol Phys 2016;95(5):1535–1543. doi:10.1016/j.ijrobp.2016.03.041 [PubMed: 27325476]
28. Fager M, Toma-Dasu I, Kirk M, et al. Linear energy transfer painting with proton therapy: A means of reducing radiation doses with equivalent clinical effectiveness. Int J Radiat Oncol Biol Phys 2015;91(5):1057–1064. doi:10.1016/j.ijrobp.2014.12.049 [PubMed: 25832696]
29. An Y, Shan J, Patel SH, et al. Robust intensity-modulated proton therapy to reduce high linear energy transfer in organs at risk: Med Phys 2017;44(12):6138–6147. doi:10.1002/mp.12610 [PubMed: 28976574]
30. Bassler N, Jäkel O, Søndergaard CS, Petersen JB. Dose- and LET-painting with particle therapy. Acta Oncol (Madr). 2010;49(7):1170–1176. doi:10.3109/0284186X.2010.510640

31. Giantsoudi D, Grassberger C, Craft D, Niemierko A, Trofimov A, Paganetti H. Linear energy transfer-guided optimization in intensity modulated proton therapy: Feasibility study and clinical potential. Int J Radiat Oncol Biol Phys 2013;87(1):216–222. doi:10.1016/j.ijrobp.2013.05.013 [PubMed: 23790771]
32. Cao W, Khabazian A, Yepes PP, et al. Linear energy transfer incorporated intensity modulated proton therapy optimization. Phys Med Biol 2018. doi:10.1088/1361-6560/aa9a2e
33. Bai X, Lim G, Grosshans D, Mohan R, Cao W. Robust optimization to reduce the impact of biological effect variation from physical uncertainties in intensity-modulated proton therapy. Phys Med Biol 2019. doi:10.1088/1361-6560/aaf5e9
34. Inaniwa T, Kanematsu N, Noda K, Kamada T. Treatment planning of intensity modulated composite particle therapy with dose and linear energy transfer optimization. Phys Med Biol 2017. doi:10.1088/1361-6560/aa68d7
35. Fjæra LF, Li Z, Ytre-Hauge KS, et al. Linear energy transfer distributions in the brainstem depending on tumour location in intensity-modulated proton therapy of paediatric cancer. Acta Oncol (Madr). 2017. doi:10.1080/0284186X.2017.1314007
36. Giantsoudi D, Adams J, MacDonald SM, Paganetti H. Proton Treatment Techniques for Posterior Fossa Tumors: Consequences for Linear Energy Transfer and Dose-Volume Parameters for the Brainstem and Organs at Risk. Int J Radiat Oncol Biol Phys 2017. doi:10.1016/j.ijrobp.2016.09.042
37. Mohan R, Peeler CR, Guan F, Bronk L, Cao W, Grosshans DR. Radiobiological issues in proton therapy. Acta Oncol (Madr). 2017;56(11):1367–1373. doi:10.1080/0284186X.2017.1348621
38. Gu W, O'Connor D, Nguyen D, et al. Integrated beam orientation and scanning-spot optimization in intensity-modulated proton therapy for brain and unilateral head and neck tumors. Med Phys 2018. doi:10.1002/mp.12788
39. Gu W, Neph R, Ruan D, Zou W, Dong L, Sheng K. Robust Beam Orientation Optimization for Intensity-Modulated Proton Therapy. Med Phys 2019;0(ja). doi:10.1002/mp.13641
40. Beck A, Teboulle M. A Fast Iterative Shrinkage-Thresholding Algorithm for Linear Inverse Problems. SIAM J Imaging Sci 2009;2(1):183–202. doi:10.1137/080716542
41. Cisternas E, Mairani A, Ziegenhein P, Jäkel O, Bangert M. matRad – a multi-modality open source 3D treatment planning toolkit. In: IFMBE Proceedings. Vol 51.; 2015:1608–1611. doi:10.1007/978-3-319-19387-8_391
42. Wieser HP, Cisternas E, Wahl N, et al. Development of the open-source dose calculation and optimization toolkit matRad. Med Phys 2017;44(6):2556–2568. doi:10.1002/mp.12251 [PubMed: 28370020]
43. Souris K, Lee JA, Sterpin E. Fast multipurpose Monte Carlo simulation for proton therapy using multi- and many-core CPU architectures. Med Phys 2016. doi:10.1118/1.4943377
44. Huang S, Kang M, Souris K, et al. Validation and clinical implementation of an accurate Monte Carlo code for pencil beam scanning proton therapy. J Appl Clin Med Phys 2018. doi:10.1002/acm2.12420
45. Jia X, Schümann J, Paganetti H, Jiang SB. GPU-based fast Monte Carlo dose calculation for proton therapy. Phys Med Biol 2012. doi:10.1088/0031-9155/57/23/7783
46. Giantsoudi D, Schuemann J, Jia X, Dowdell S, Jiang S, Paganetti H. Validation of a GPU-based Monte Carlo code (gPMC) for proton radiation therapy: clinical cases study. Phys Med Biol 2015;60(6):2257–2269. doi:10.1088/0031-9155/60/6/2257 [PubMed: 25715661]
47. Grégoire V, Mackie TR. State of the art on dose prescription, reporting and recording in Intensity-Modulated Radiation Therapy (ICRU report No. 83). Cancer/Radiotherapie. 2011;15(6–7):555–559. doi:10.1016/j.canrad.2011.04.003
48. Giantsoudi D, Unkelbach J, Botas P, Grassberger C, Paganetti H. Can Robust Optimization for Range Uncertainty in Proton Therapy Act as a Surrogate for Biological Optimization? Int J Radiat Oncol 2017. doi:10.1016/j.ijrobp.2017.06.253
49. Gu W, Ruan D, O'Connor D, et al. Robust optimization for intensity-modulated proton therapy with soft spot sensitivity regularization. Med Phys 2019. doi:10.1002/mp.13344

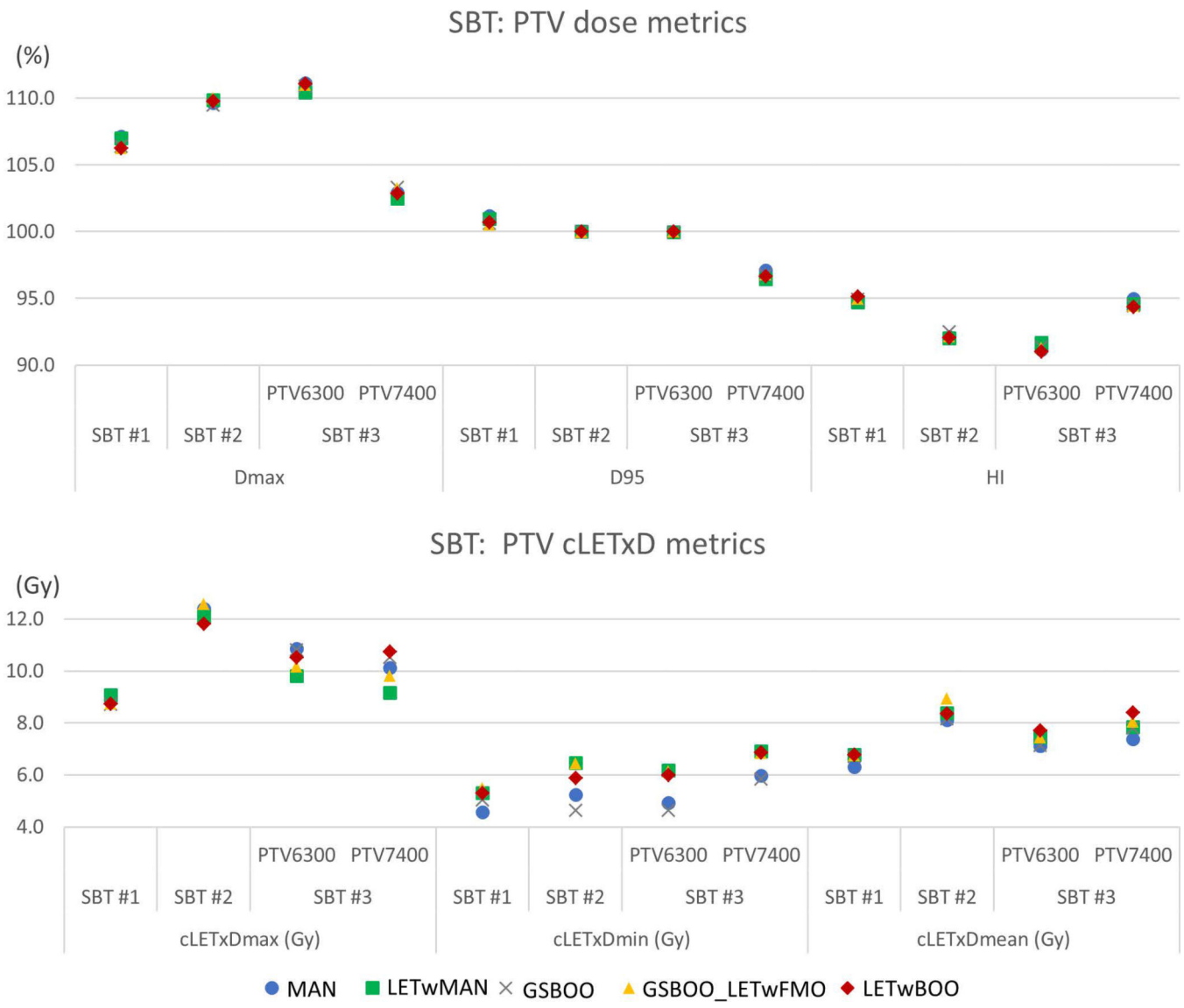

Figure 1.

The comparison of PTV dose and cLET×D metrics between MAN, LETwMAN, GSBOO, GSBOO_LETwFMO and LETwBOO for the three SBT patients.

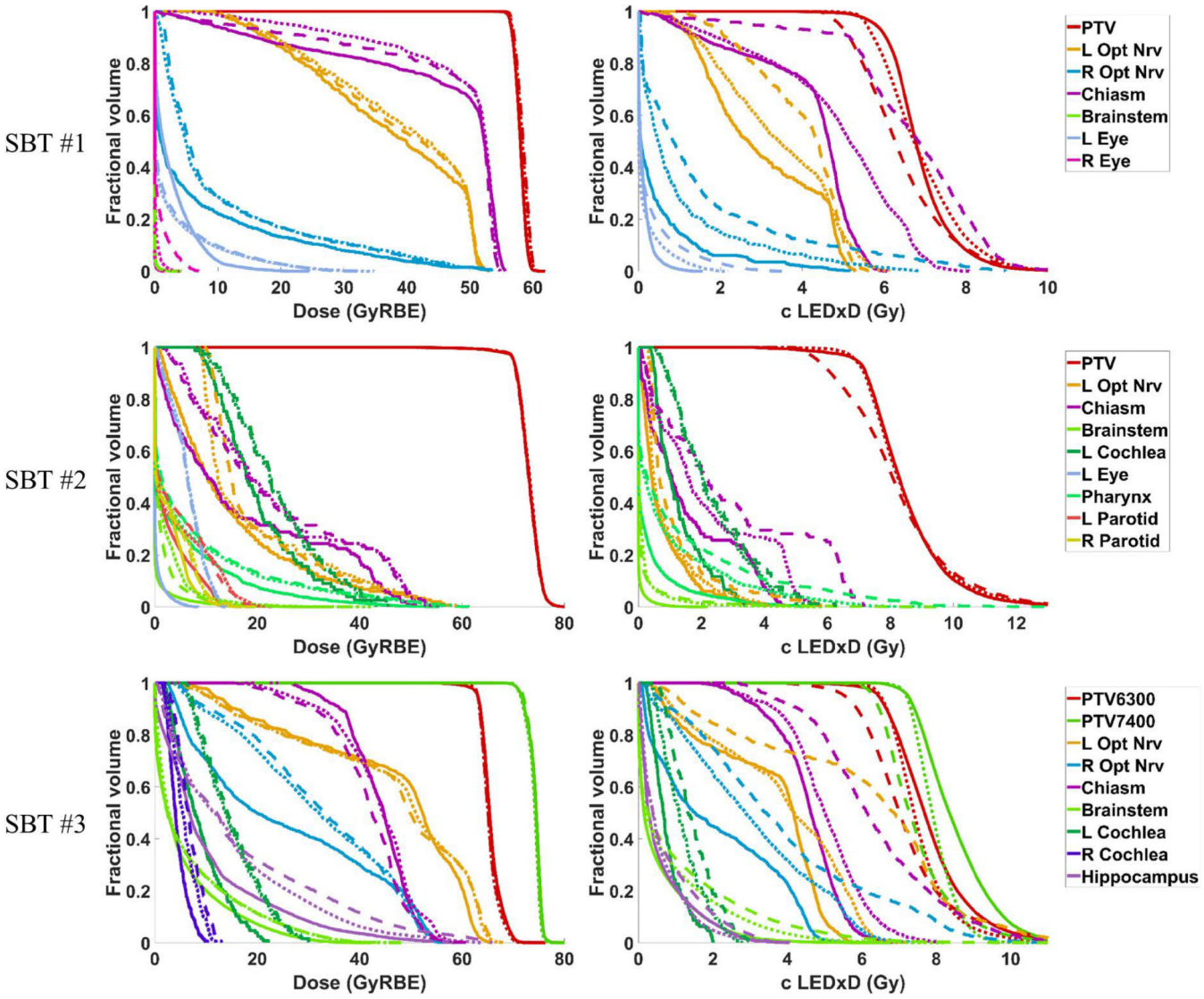

Figure 2.

Comparison of dose and cLET×D between LETwBOO (solid), LETwMAN (dotted) and MAN (dashed) for the SBT patients. Left column is the dose volume histogram and right column is the cLET×D volume histogram.

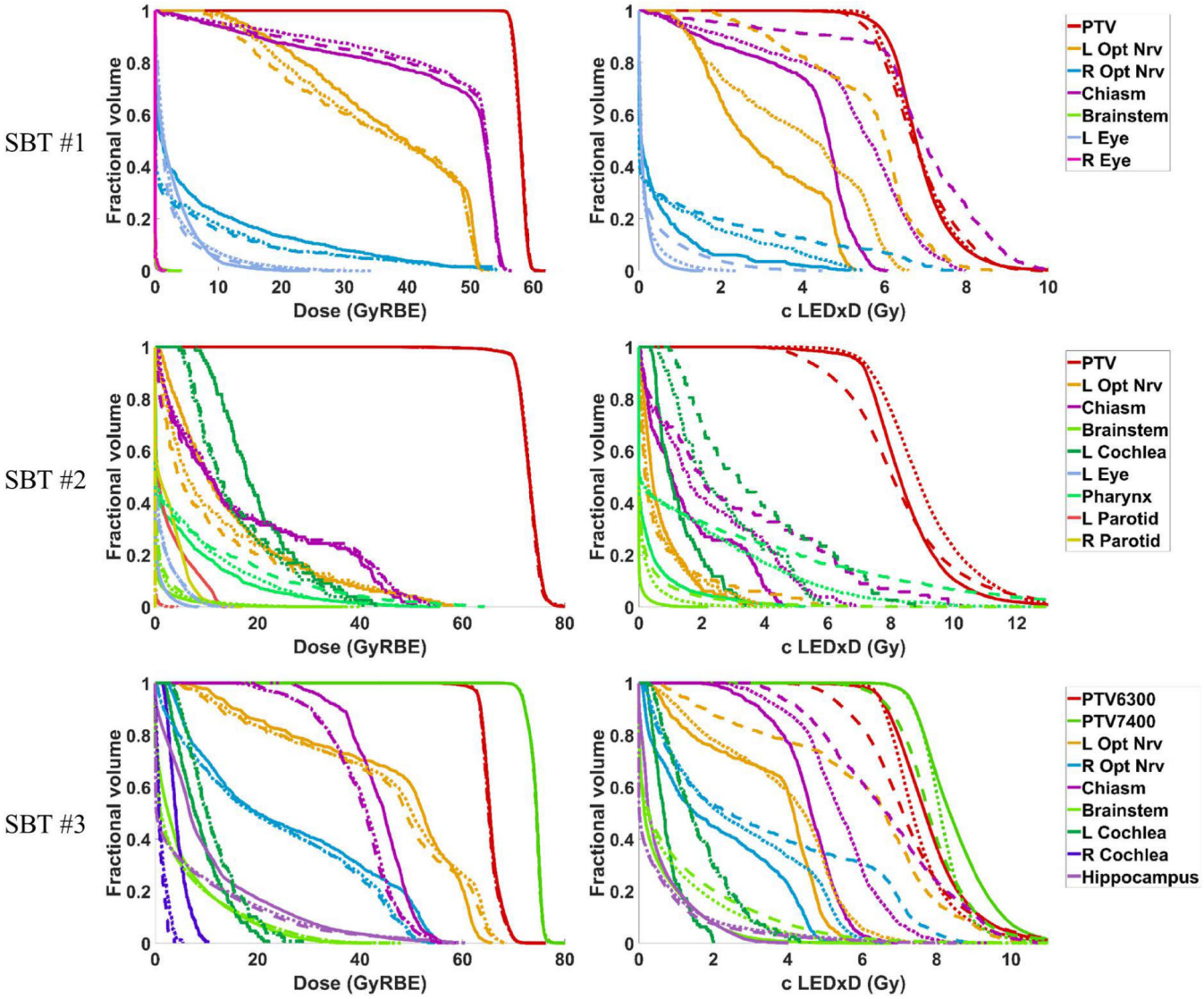

Figure 3.

Comparison of dose and cLET×D between LETwBOO (solid), GSBOO_LETwFMO (dotted) and GSBOO (dashed) for the SBT patients. Left column is the dose volume histogram and right column is the cLET×D volume histogram.

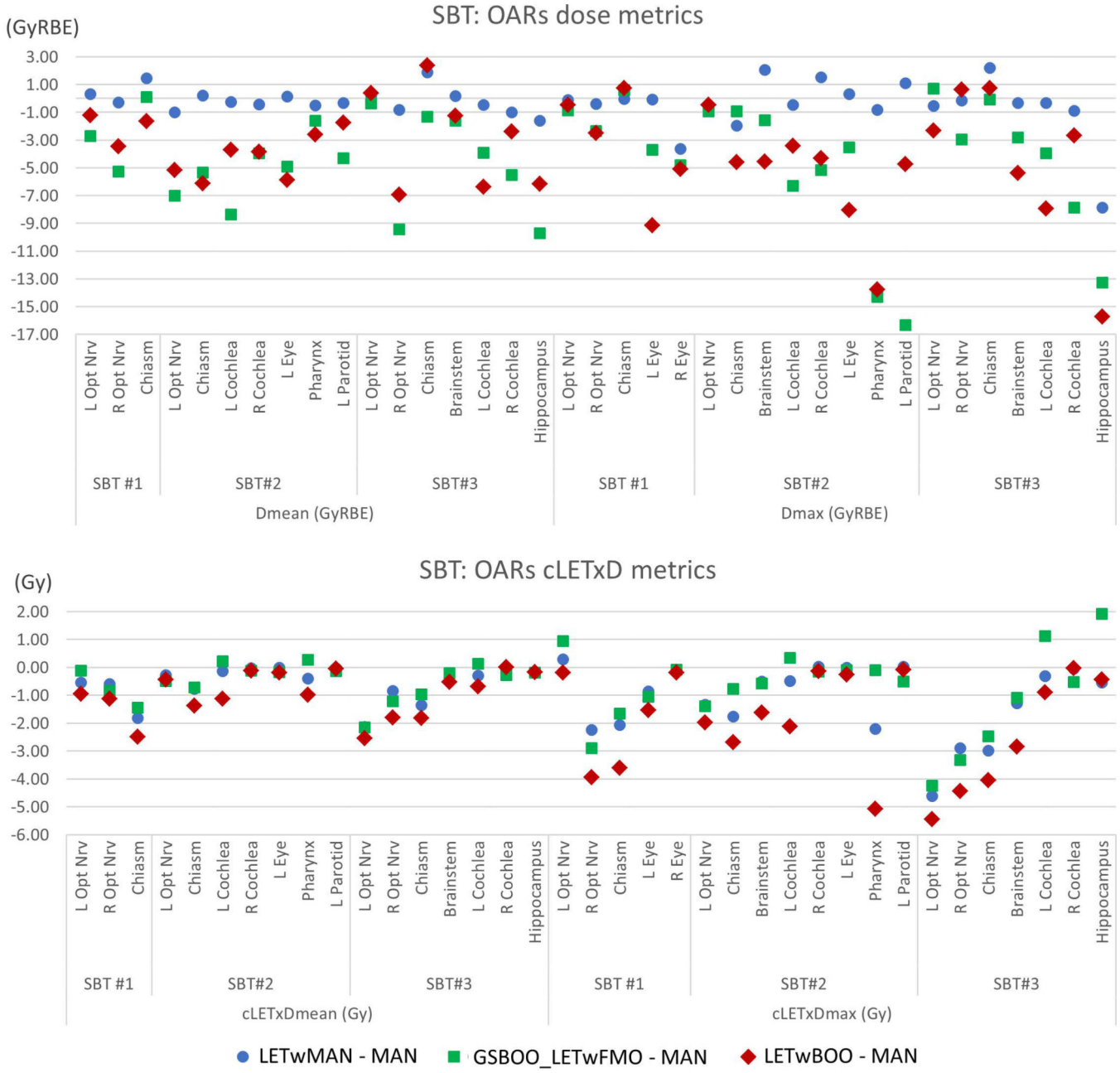

Figure 4.

The difference of OAR dose and cLET×D metrics of LETwMAN, GSBOO_LETwFMO and LETwBOO from MAN for the three SBT patients. A negative sign represents a reduction from the MAN plan and a positive sign represents an increase.

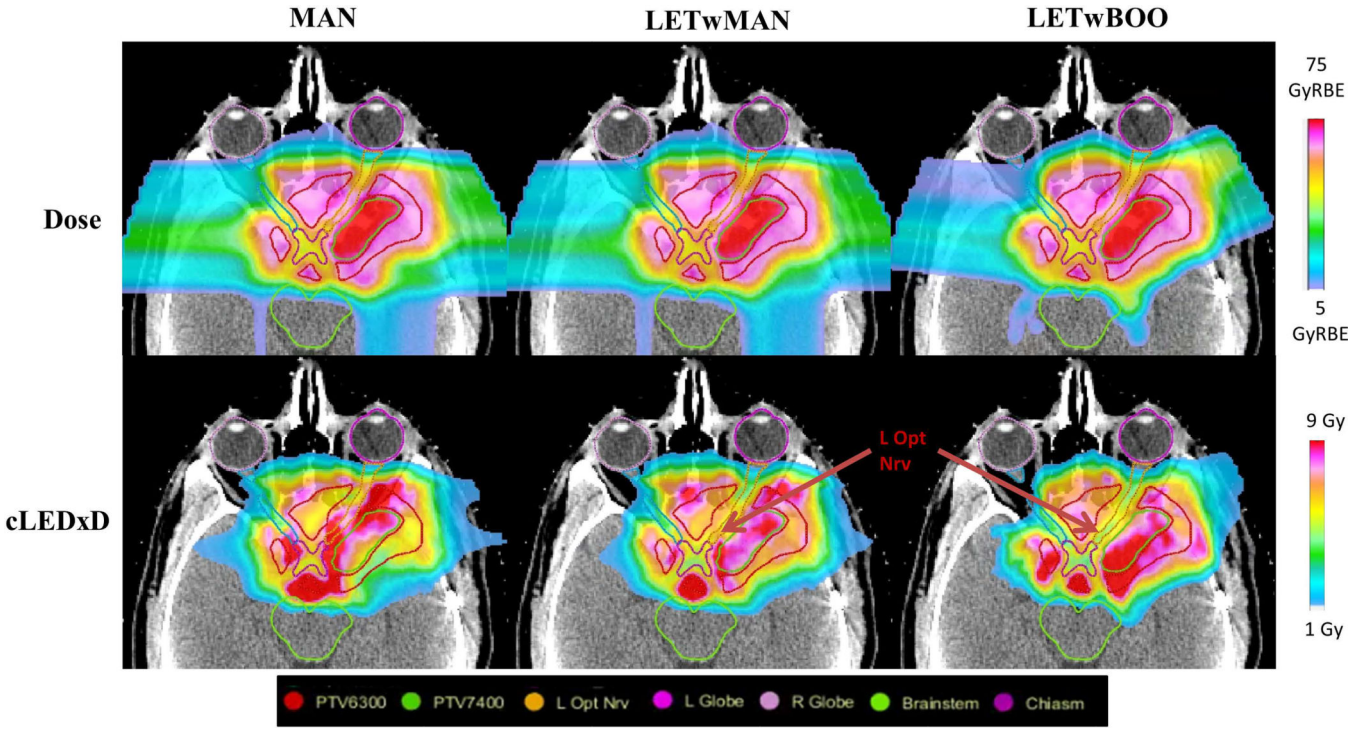

Figure 5.
Isodose and iso-cLET×D for the SBT#3 patient between MAN, LETwMAN and LETwBOO plans.

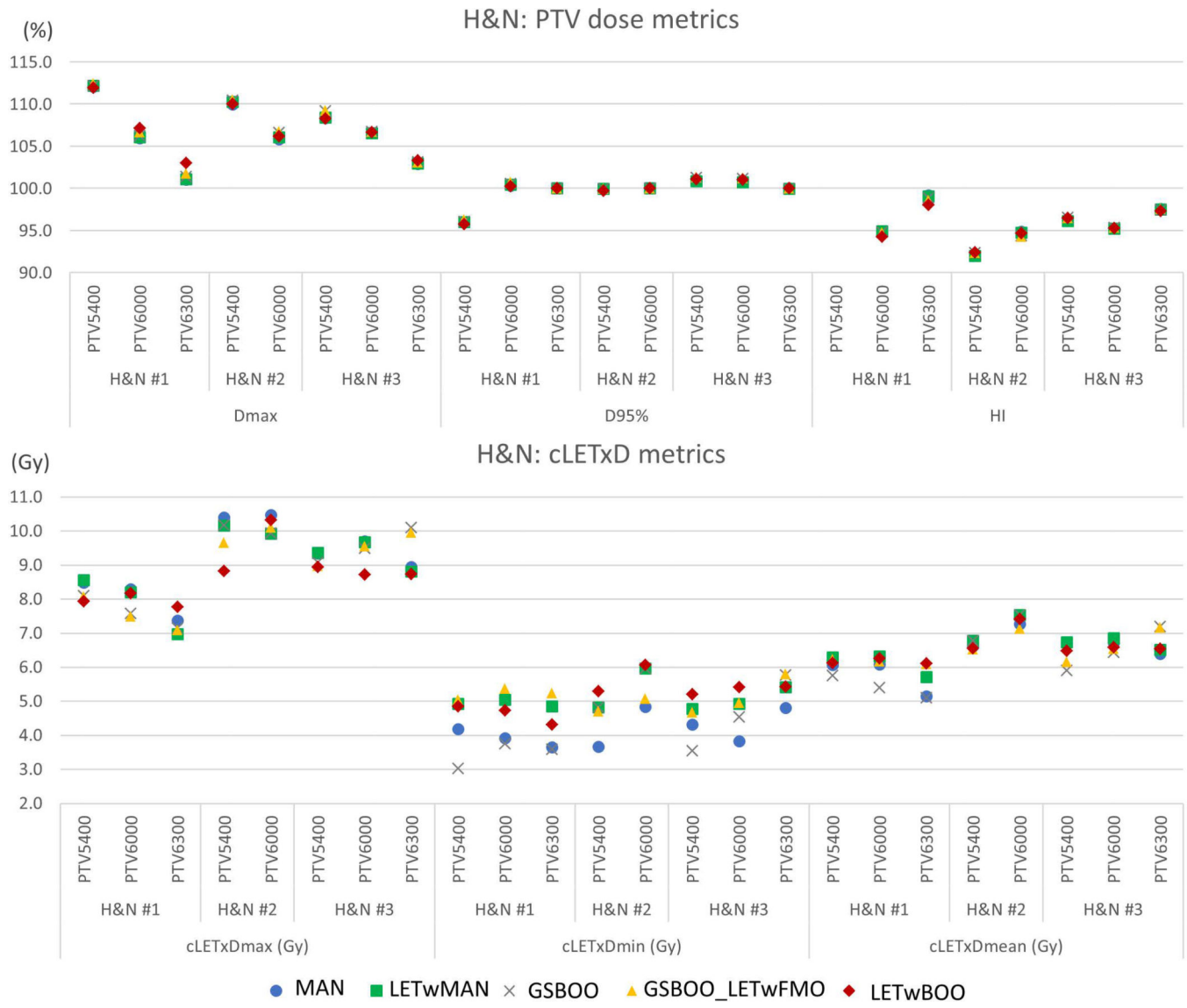

Figure 6.

The comparison of PTV dose and cLET×D metrics between MAN, LETwMAN, GSBOO, GSBOO_LETwFMO and LETwBOO for the three H&N patients.

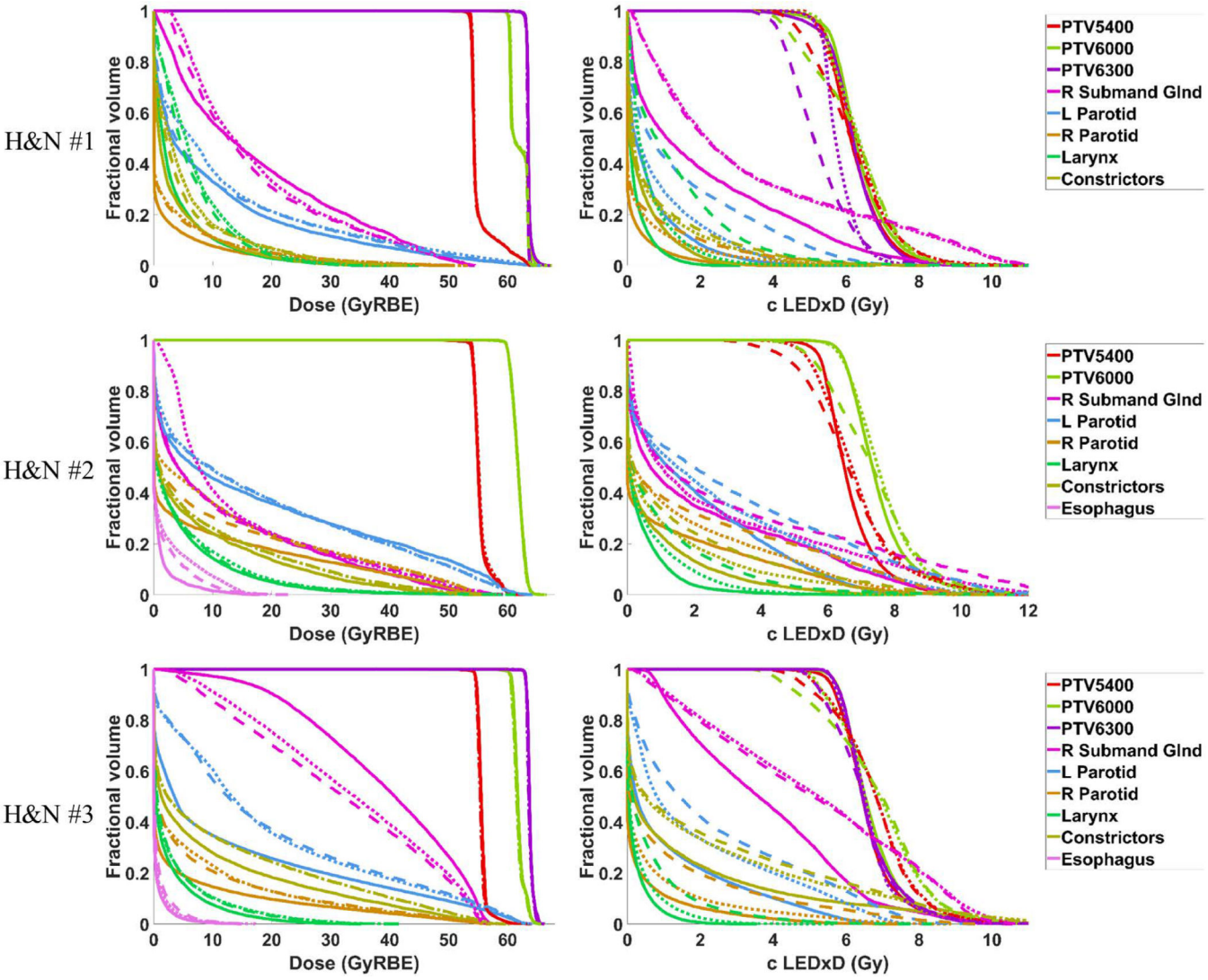

Figure 7.

Comparison of dose and cLET×D between LETwBOO (solid), LETwMAN (dotted) and MAN (dashed) for the H&N patients. Left column is the dose volume histogram and right column is the cLET×D volume histogram.

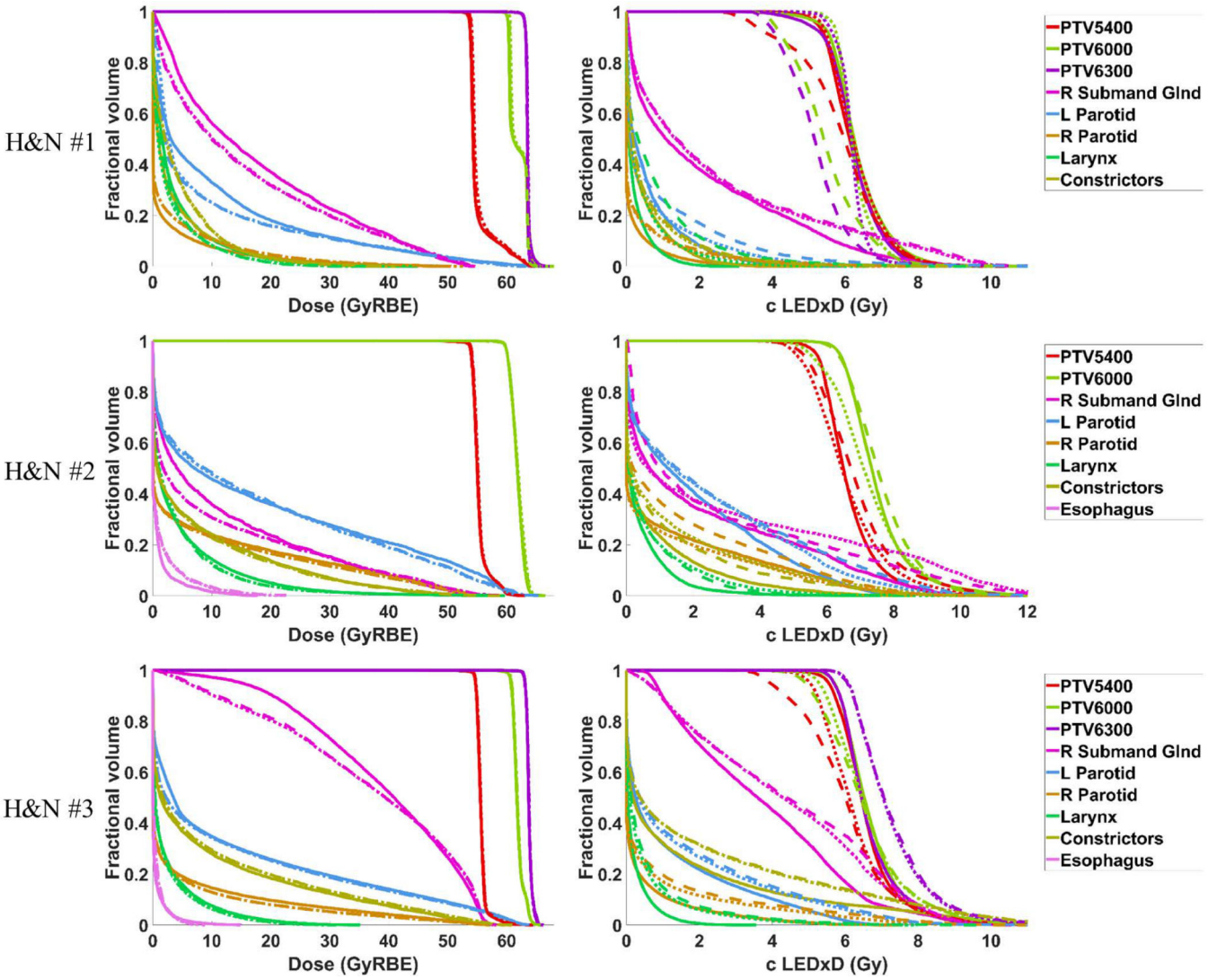

Figure 8.

Comparison of dose and cLET×D between LETwBOO (solid), GSBOO_LETwFMO (dotted) and GSBOO (dashed) for the H&N patients. Left column is the dose volume histogram and right column is the cLET×D volume histogram.

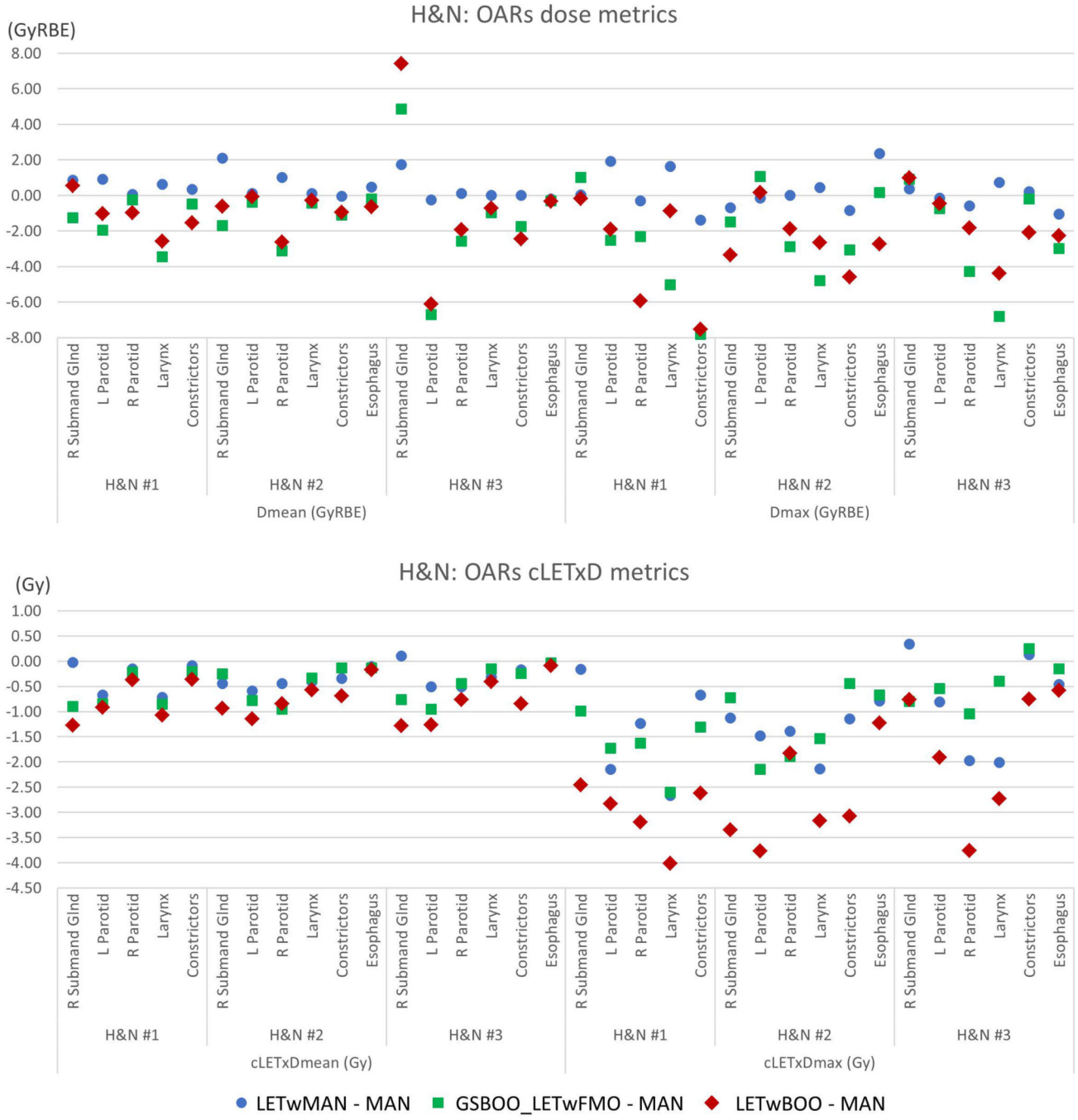

Figure 9.

The difference of OAR dose and cLET×D metrics of LETwMAN, GSBOO_LETwFMO and LETwBOO from MAN for the three H&N patients. A negative sign represents a reduction from the MAN plan and a positive sign represents an increase.

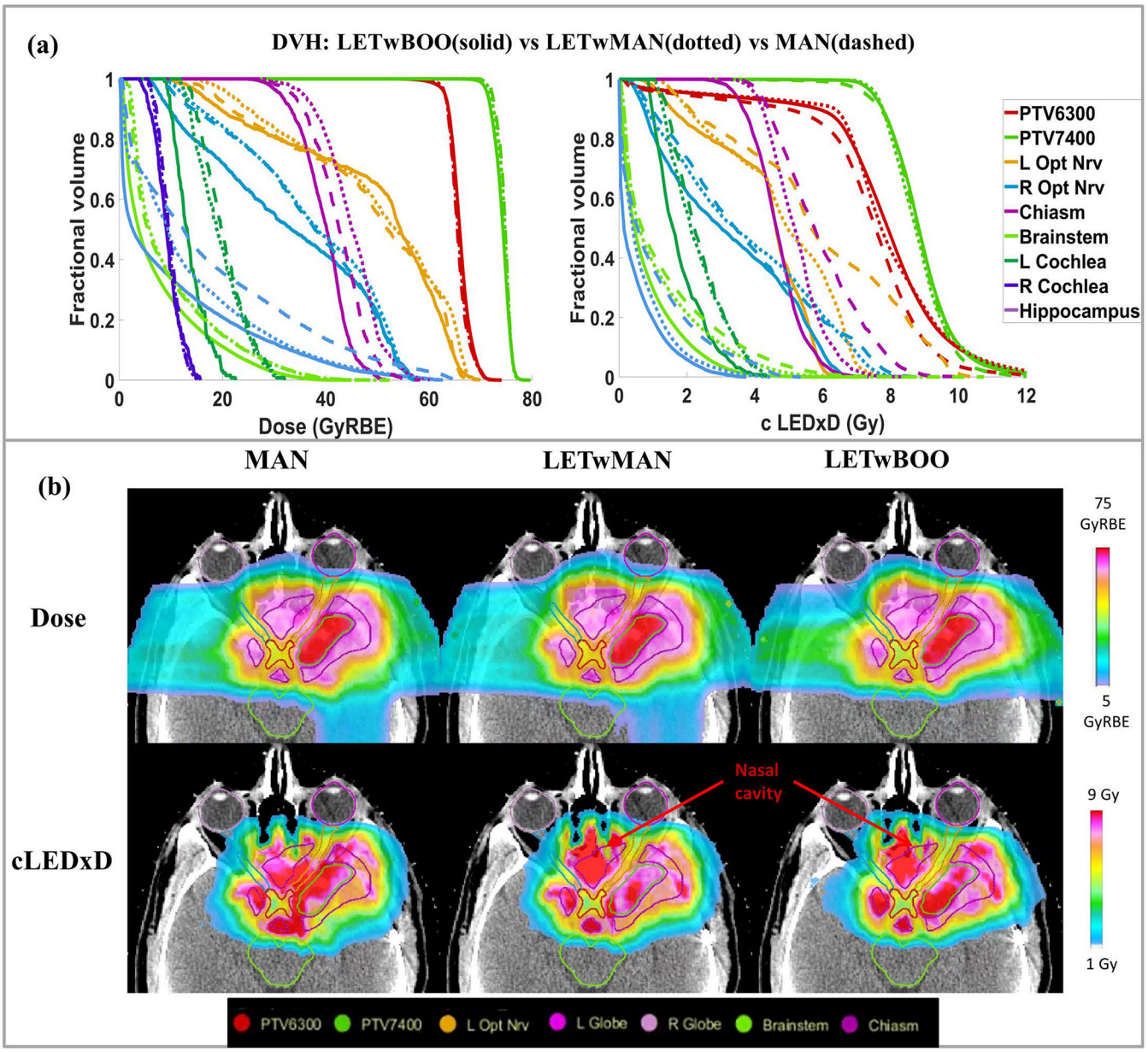

Figure 10.

Plans optimized by MCsquare. (a) Comparison of dose and cLET×D between LETwBOO (solid), LETwMAN (dotted) and MAN (dashed) for the SBT#3 patients. (b) Isodose and iso-cLET×D for the SBT#3 patient between MAN, LETwMAN and LETwBOO plans.

Table I.

Prescription doses, PTV volumes and average number of spots per beam for each patient.

Case		Prescription Dose (GyRBE)	CTV Volume (cc)	Average Spots Number per Beam
SBT #1		56	66.80	2537
SBT #2		70	70.26	2650
SBT #3	PTV6300	63	128.86	4071
	PTV7400	74	26.58	
H&N #1	PTV5400	54	257.41	10065
	PTV6000	60	274.38	
	PTV6300	63	121.52	
H&N #2	PTV5400	54	205.76	10077
	PTV6000	60	210.43	
H&N #3	PTV5400	54	206.10	9433
	PTV6000	60	173.56	
	PTV6300	63	21.20	

Table II.

Acronyms of different methods and the comparison

Acronym	Initial optimization			Re-optimized with cLET×D constraint?
	Beam selection method	Physical dose constraint?	cLET×D constraint?	
MAN	Manual selection	Yes	No	No
LETwMAN	Manual selection	Yes	No	Yes
GSBOO	Group sparsity	Yes	No	No
GSBOO_LETwFMO	Group sparsity	Yes	No	Yes
LETwBOO	Group sparsity	Yes	Yes	No

Table III.

Optimization time and selected beam angles for each patient.

Case	Dose, LET calculation time on matRad (min)	BOO runtime (min)		Selected beam angles (gantry, couch)		
		GSBOO	LETwBOO	MAN	GSBOO	LETwBOO
SBT #1	11	21	31	(60,275)(270,0) (90,0)	(303,62)(97,324) (42,37)	(288,45)(123,331) (42,37)
SBT #2	16	25	46	(60,275)(270,0) (90,0)(180,0)	(62,339)(341,19) (300,353)(17,46)	(95,281)(60,332) (137,18)(276,342)
SBT #3	21	31	56	(60,275)(270,0) (90,0)(180,0)	(66,0)(84,0) (270,342) (316,314)	(268,84)(276,0) (67,20) (33,66)
H&N #1	56	70	101	(0,0)(160,0) (200,0)	(51,320)(154,293) (330,321)	(188,45)(38,20) (330,321)
H&N #2	58	55	73	(0,0)(160,0) (200,0)	(322,20)(167,296) (212,23)	(167,296)(212,23) (324,301)
H&N #3	55	62	89	(0,0)(160,0) (200,0)	(149,348)(193,27) (41,50)	(149,348)(188,45) (31,76)